Massachusetts Institute of Technology

Possibilities in GPD Physics with Increased CLAS12 *Precision*

Timothy B. Hayward

Workshop on the Physics Program with High Luminosity Facilities

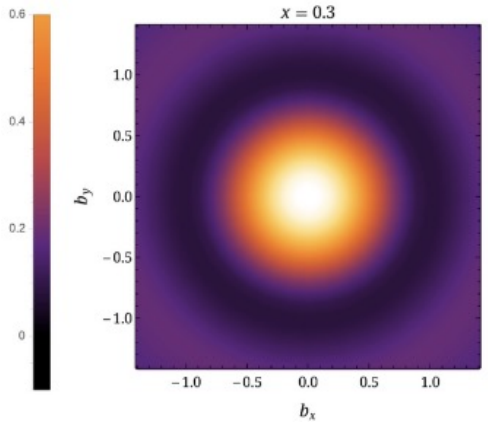
October 7th, 2026

Nucleon Structure through Generalized Parton Distributions

- Generalized Parton Distributions (GPDs) unify form factors and parton distribution functions and provide a more complete 3D picture of the nucleon.
- Give access to information on the correlations between transverse position and longitudinal momentum of quarks and gluons inside the nucleon.
- Accessible experimentally through measurements of exclusive processes such as Deeply Virtual Compton Scattering (DVCS) or Deeply Virtual Meson Production (DVMP).

Nucleon Polarization	Quark Polarization: Unpolarized (U)	Quark Polarization: Longitudinally Polarized (L)	Quark Polarization: Transversely Polarized (T)
U	H		$\bar{E} = 2\tilde{H}_T + E_T$
L		$\widetilde{H}$	$\widetilde{E}_T$
T	E	$\widetilde{E}$	$H_T, \widetilde{H}_T$

Nucleon Tomography



H.W. Lin, Phys. Rev. Lett. 127 (2021) 182001.

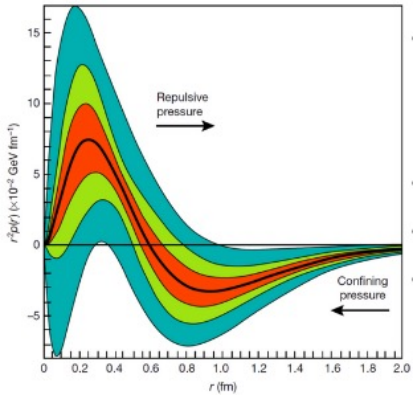
Contributions to the total nucleon spin

$$\frac{1}{2} = \frac{1}{2}\Delta\Sigma + \Delta L + \Delta G$$

X. Ji, Phys. Rev. Lett. 78,610 (1997)

1. Quark contribution; not the main contribution → spin crisis.
2. Quark's orbital angular momentum, accessed through GPDs.
3. Gluon spin contributions.

Gravitational Form Factors



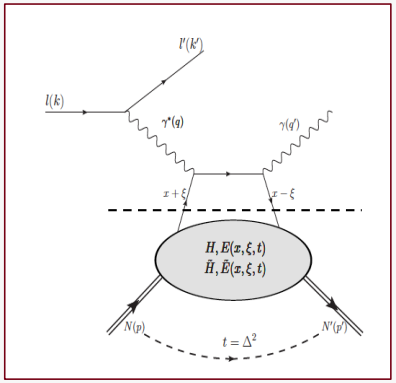
V. D. Burkert et al., Nature 557.7705 (2018): 396

- Mass/energy distribution inside the nucleon.
- Nucleon mass radius.
- Shear forces and pressure distributions.

DVCS and the Mechanical Structure of the Proton

DVCS provides access to CFFs

- In DVCS the hard photon interaction factorizes from the nonperturbative nucleon structure described by chiral even GPDs.
- DVCS observables constrain the corresponding CFFs through interference with BH.

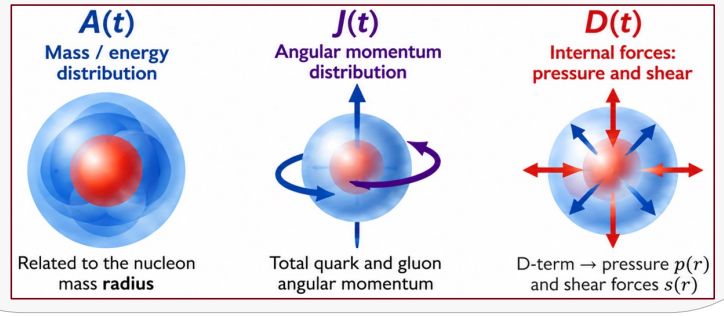


- The real part of $\mathcal{H}$ provides sensitivity to the D-term through a dispersion relationship.

GPD moments relate to GFFs

- Matrix elements of the QCD energy-momentum tensor are parametrized by gravitational form factors (GFFs).
- The GFFs encode fundamental properties of the nucleon:

$$\int_{-1}^{1} dx x H(x,\xi,t) = A(t) + \xi^2 D(t)$$

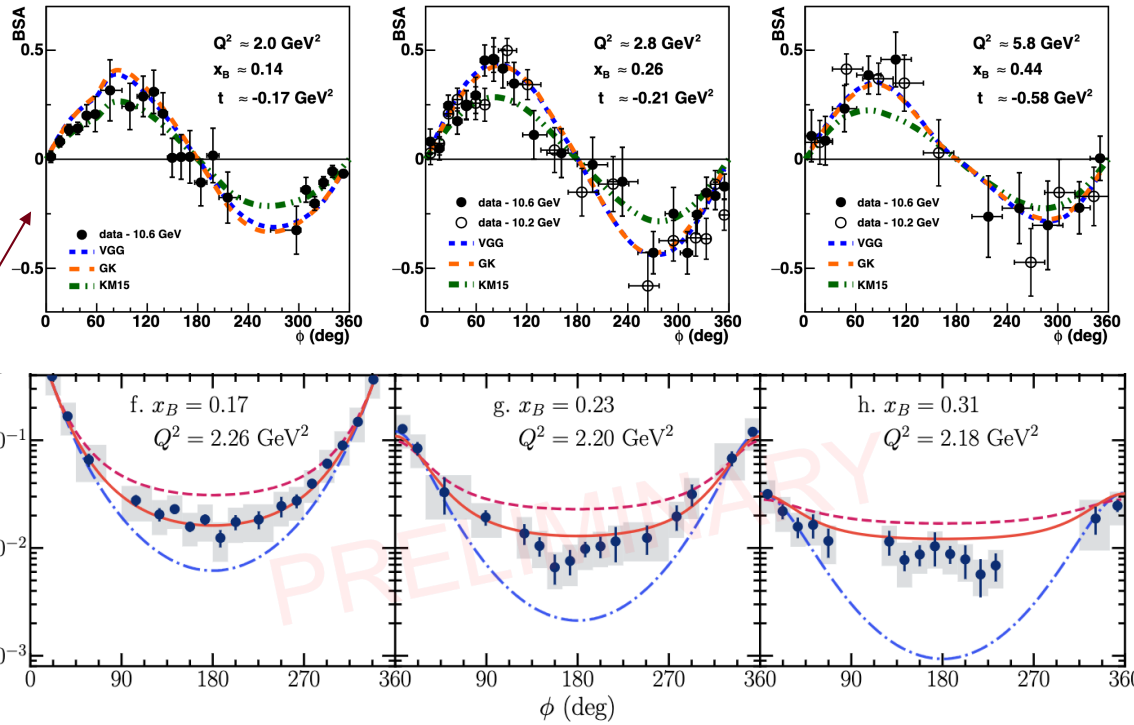


DVCS Observables → CFFs → D(t) → p(r), s(r)

pDVCS Measurements in Hall B

Many generations of complementary DVCS observables at CLAS and CLAS12

Year	Measurement	Reference	arXiv
2001	BSA	PRL **87**, 182002	hep-ex/0107043
2006	TSA	PRL **97**, 072002	hep-ex/0605012
2008	BSA	PRL **100**, 162002	0711.4805
2009	BSA	PRC **80**, 035206	0812.2950
2015	TSA	PRL **114**, 032001	1410.6615
2015	BSA,TSA,DSA	PRD **91**, 052014	1501.07052
2015	σ	PRL **115**, 212003	1504.02009
2018	σ	PRC **98**, 045203	1810.02110
2023	BSA (CLAS12)	PRL **130**, 211902	2211.11274
2026	σ (CLAS12)	submitted to PRC	2608.20585



CLAS12:

- >2000 BSA and >1300 4-fold differential BSA/σ measurements extending the Q^2-x_B reach in the valence region.
- Greatly enhanced sensitivity to Re and Im parts of $\mathcal{H}$ with indications of tension in previously unexplored phase space.
- Data represents ~1/2 collected statistics.

High Luminosity Extends the |t| Lever Arm

Mechanical structure needs a broad |t| lever arm
(access t-dependence of D term)

↓

Factorization regime: $\frac{|t|}{Q^2} < 0.2^{*} \leftrightarrow Q^2 > 5|t|$

* preferences vary

↓

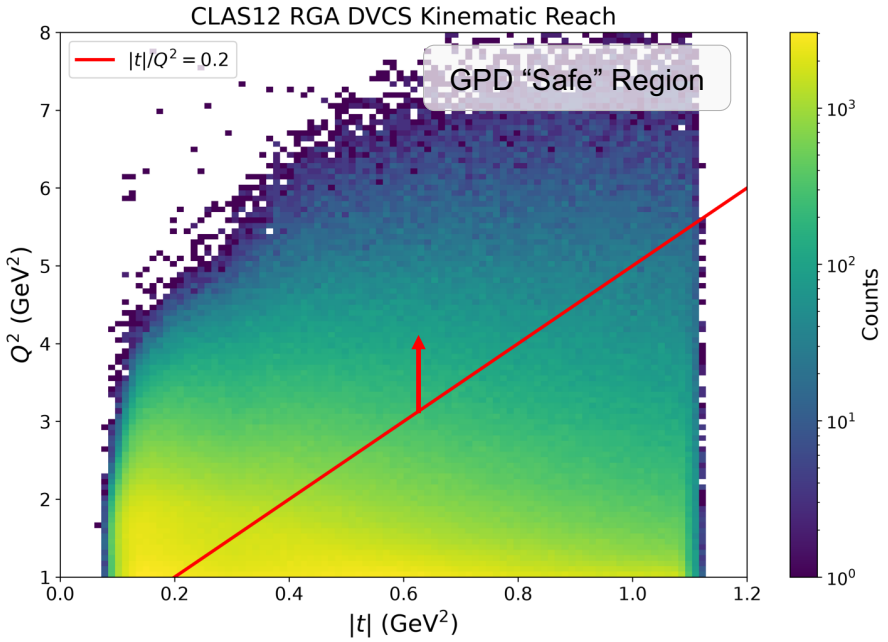
Large |t| therefore requires large Q^2:

$|t| = 0.5\ \mathrm{GeV}^2 \rightarrow Q^2 > 2.5\ \mathrm{GeV}^2$

$|t| = 1.0\ \mathrm{GeV}^2 \rightarrow Q^2 > 5.0\ \mathrm{GeV}^2$

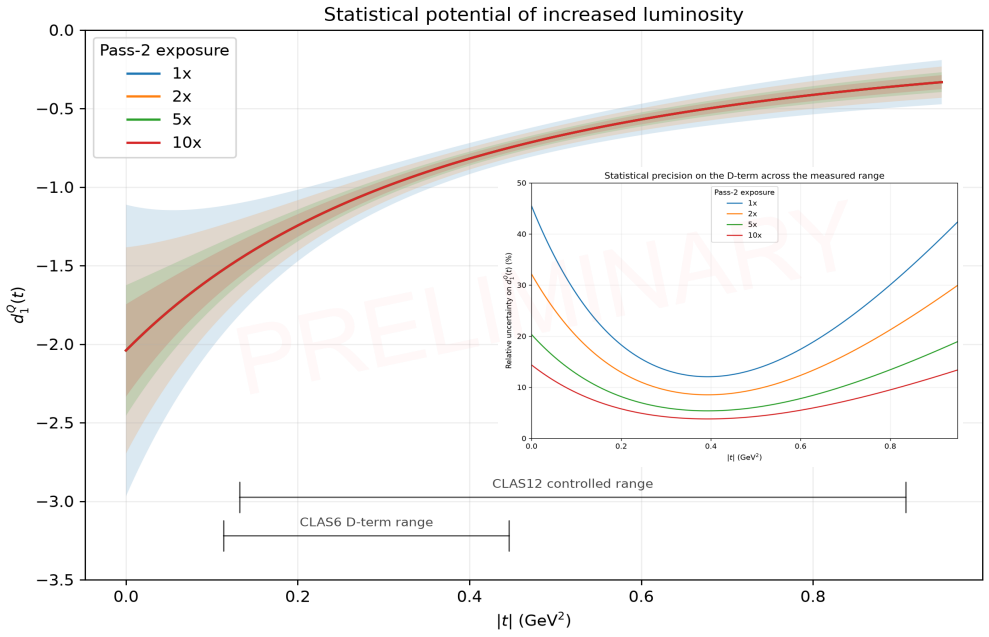
↓

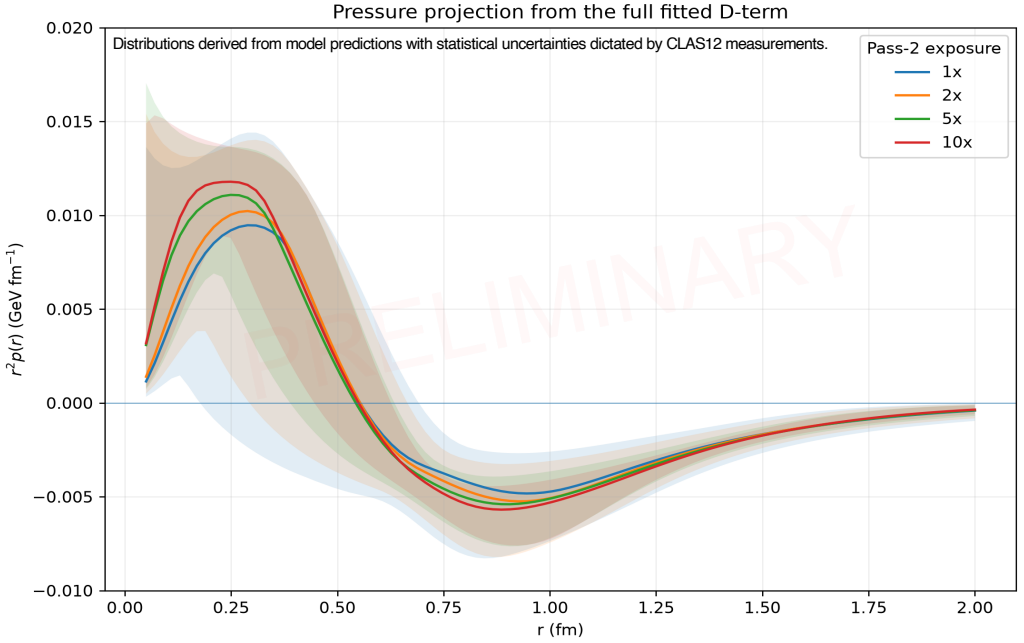
Cross sections fall rapidly with Q^2.
High luminosity could buy new controlled reach in |t|,
not just smaller error bars.



From DVCS to pressure: what luminosity buys

DVCS Observables → CFFs → D(t) → p(r), s(r)

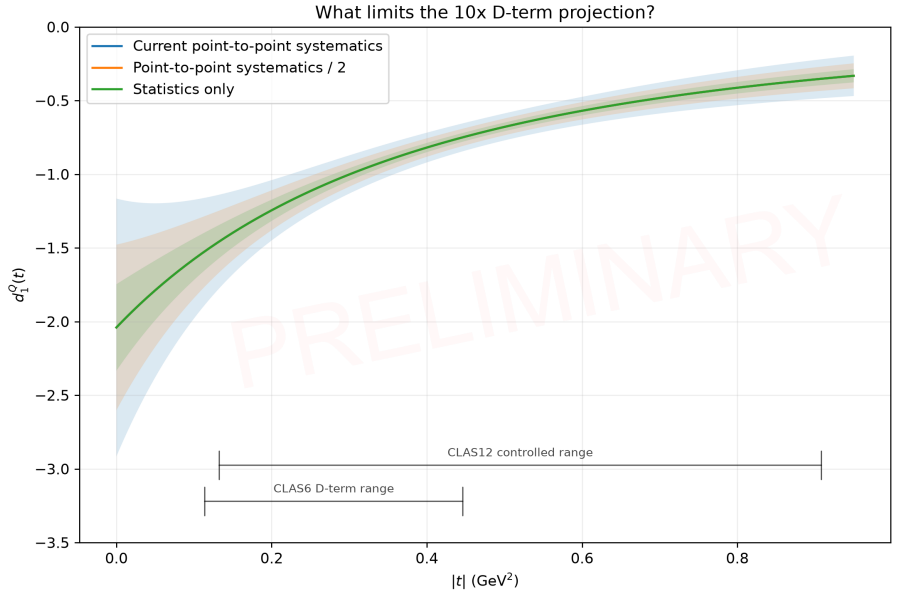


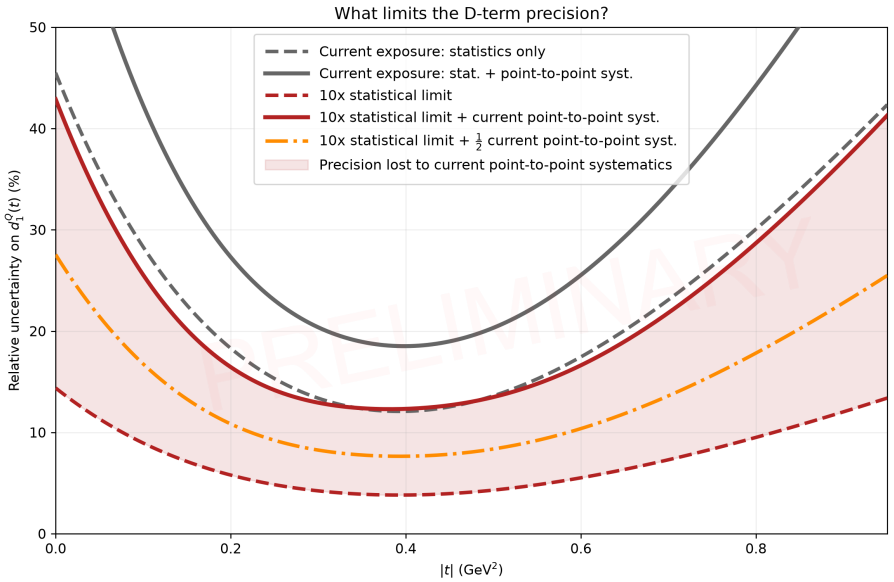


More statistics constrain D(t) and lead to sharper determinations of the proton's internal distributions.

But Luminosity Alone is Not Enough

At high exposure, point-to-point systematics become the floor.





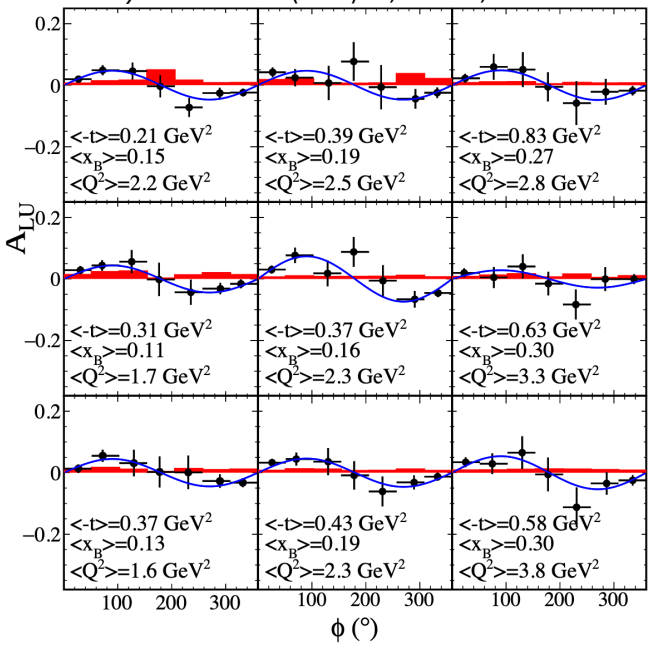
- Current CLAS12 DVCS measurements have $\sigma_{stat} \sim \sigma_{sys}$. Future measurements quickly become systematics limited.
- Systematic improvement is attainable: acceptance, π^0 background subtraction, efficiencies (statistics limited!) etc.

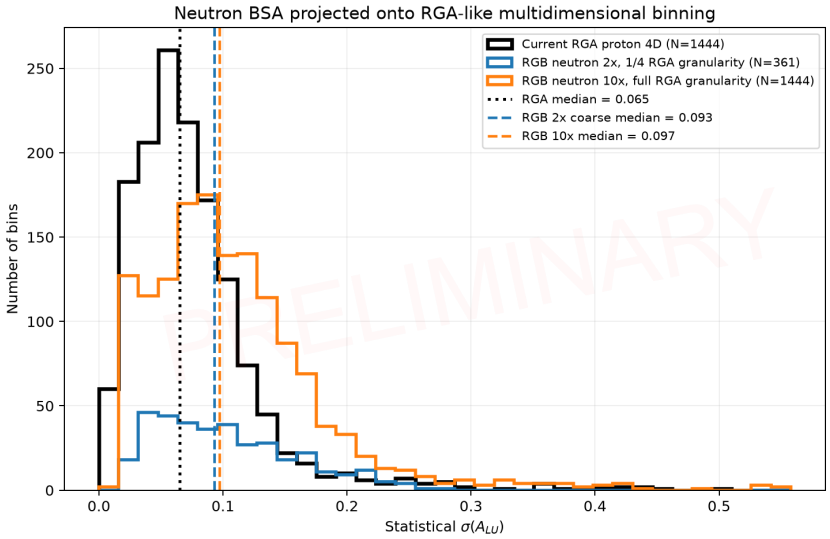
Unpolarized nDVCS

- CLAS12 has published the first measurement of DVCS on the neutron with detection of the active neutron.
- Current measurement limited to 1D binning in ϕ and either |t|, Q^2 or x_B.
- Projecting onto the existing RGA 4D (Q^2, x_B, t, ϕ):
  - 10x statistics → median $\sigma(A_{LU}) \sim 0.1$, about 1.5x the current RGA 4-D precision

- High luminosity could move nDVCS from 1-D projections toward precise multidimensional binning comparable with current pDVCS measurements.

Phys.Rev.Lett. 133 (2024) 21, 211903; 2406.15539





Flavor Separation and J_q

$$J_{q_v} = \frac{1}{2}\int_0^1 dx x[H_v^q(x,\xi,0) + E_v^q(x,\xi,0)]$$

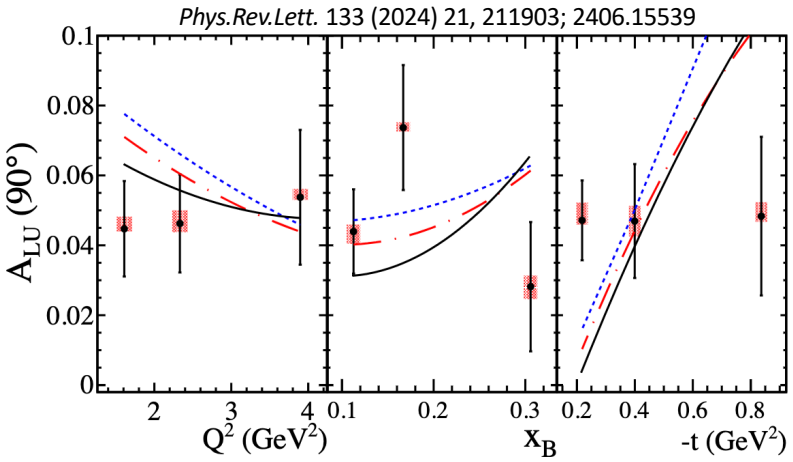
simplified DFJK-inspired valence-E parameterization

$$E_v^q(x) = N_q x^{-0.55}(1-x)^{\beta_q}$$

$$E(x,0,t) = E(x,0,0)e^{B_E t}$$

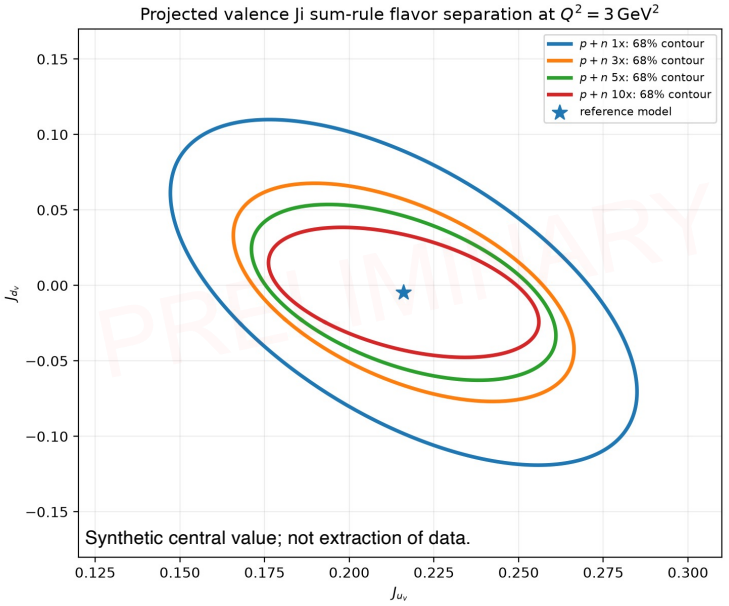
DVCS statistics constraint β_u and β_d

- Proton + neutron DVCS provides complementary sensitivity to E^u and E^d enabling flavor separation through the Ji sum rule.
- High precision substantially tightens the (model dependent, preliminary) flavor separated constraint, 1x → 5x: $\sigma(J_u)$ = 0.045 → 0.030, $\sigma(J_d)$ = 0.075 → 0.038.
- Already with RGA+RGB alone projected precision approaches the scale of modern valence-GPD determinations and future EIC/EicC possibilities.



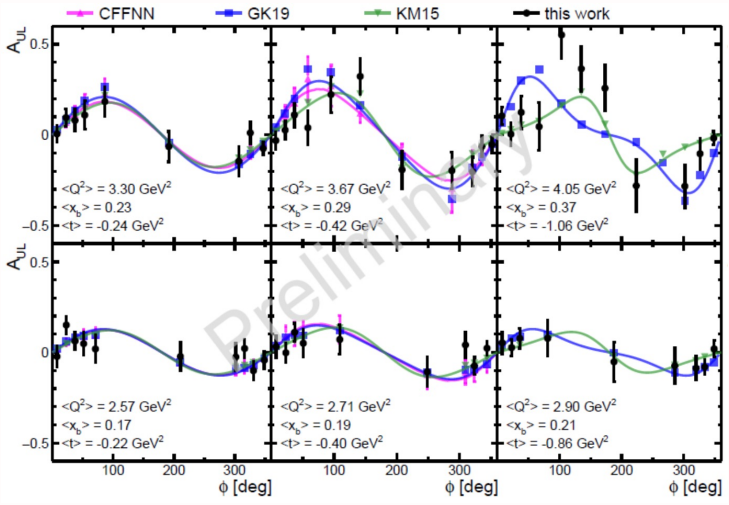
VGG model predictions for combinations of J_u and J_d yielding the best match to data.

J_u = 0.35, J_d = 0.05
J_u = -0.20, J_d = 0.15
J_u = -0.45, J_d = 0.20



Polarized DVCS: Longitudinal RGC + Transverse RGH

RGC: longitudinal target — A_{UL} and A_{LL}



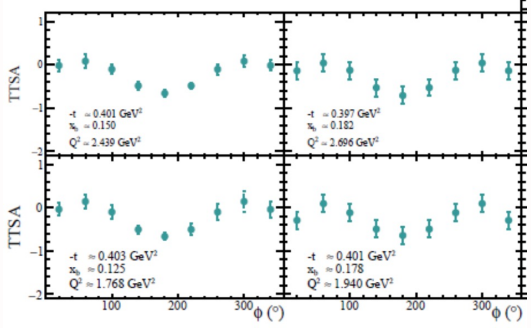
First CLAS12 longitudinal-target pDVCS asymmetries; even the 1-D result remains statistics dominated.

S. Polcher Rafael, PoS(QNP2024)070 (1-D A_{UL})

RGH: transverse target — direct leverage on E

Projections for pDVCS

- 100 days of beam time
- L = 5 x10^{33} cm^{-2} s^{-1}
- 252 bins in (Q^2, x_B, -t, ϕ)
- VGG model
- Different values of J_u, J_d



- **A_{UT} gives the key transverse-target constraint on GPD E.**
- The approved program is intrinsically 4-D in x_B, Q^2, t and ϕ.
- RGC + RGH provide complementary CFF combinations rather than redundant asymmetries.
- RGC nDVCS: first neutron A_{UL}/A_{LL} (E sensitivity), but present statistics may be insufficient for a publishable multidimensional result.

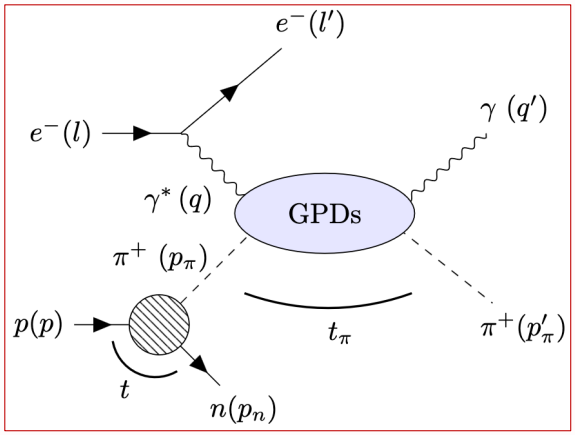
N. Pilleux, Ph.D. thesis (2024), RGC p/nDVCS; E12-12-010 / RGH proposal, Fig. 19.

pDVCS + nDVCS, longitudinal + transverse spin → substantially stronger H, E, $\tilde{H}$, $\tilde{E}$ constraints and flavor separation.

Pion GPDs through Sullivan DVCS

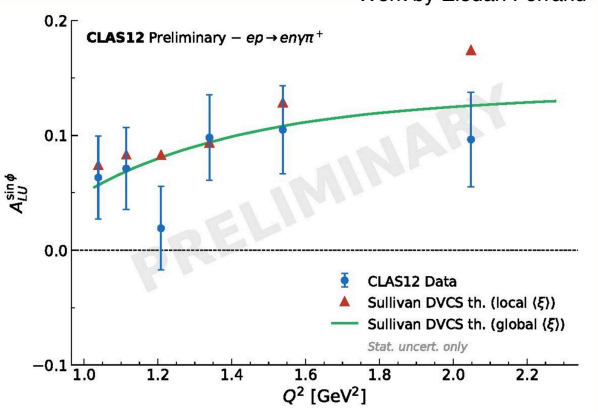
Sullivan DVCS Mechanism

- No free pion target → use the pion cloud ($p \rightarrow n + \pi^+$).
- Near the pion pole (small –t): access to pion GPDs and 3D partonic structure.
- Pion is spin-0 → simple GPD structure.



CLAS12 Preliminary Result

Work by Elouan Ferrand



$$A_{LU}^{\sin\phi} \approx 0.080 \pm 0.011\ (\text{stat})$$
(preliminary)

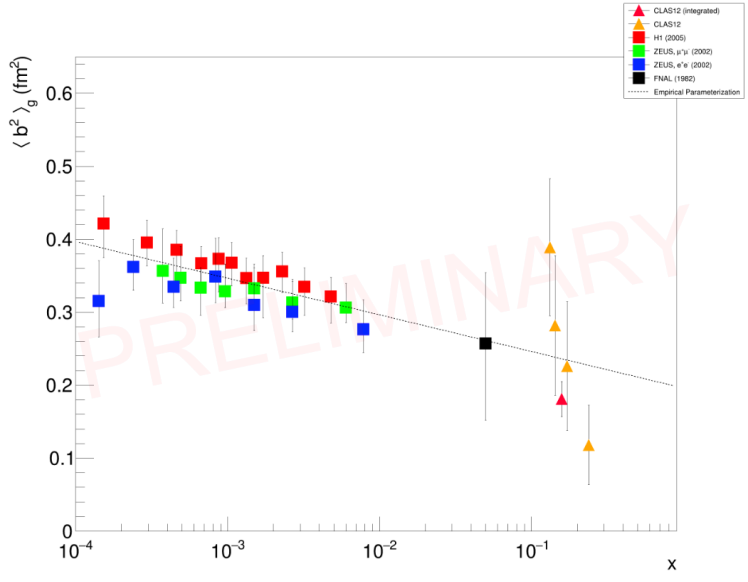
- Measurement using only a subset of unpolarized H_2 data. *Strongly* prefers "outbending" torus configuration.

Why high luminosity?

- Sullivan DVCS cross section << proton DVCS cross section.
- Exclusive four-body final state (e',γ,π^+,n).
- Current result is largely kinematically integrated, ~30,000 events.
- Accessing pion GPDs will require differential measurements.
- Increased precision may enable detailed pion tomography!

Exclusive ϕ Production: Gluon and Mechanical Structure

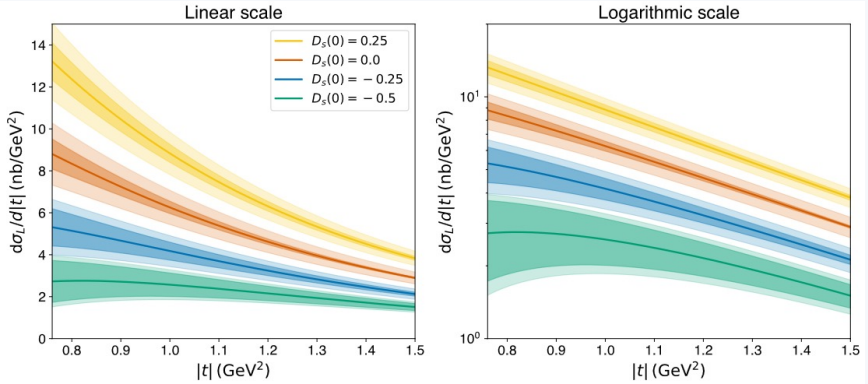
RGA: gluon imaging in the valence region



t-slope → transverse gluon distribution; first valence-region gluonic-radius extraction

P. Moran, MIT Ph.D. thesis (2025), Fig. 5.18;

High-luminosity opportunity: strong D-term



- Near-threshold ϕ: $D_s(t)$ changes the low-|t| shape.
- Narrow Q², W and t selections make this intrinsically statistics hungry.
- Original analysis used ~½ of collected RGA; current reconstruction should already provide a much larger baseline.
- See Bhawani and Henry's talks.

Hall C E12-25-007 proposal, Fig. 4 (strangeness D-term sensitivity).

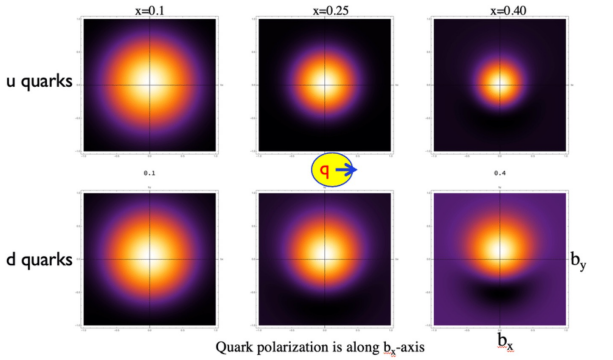
High luminosity converts an established gluon-imaging channel into a possible flavor-resolved mechanical-structure measurement.

Nucleon Structure through (Chiral Odd) Generalized Parton Distributions

- Chiral odd GPDs encode how transversely polarized quark spins are distributed in position and momentum inside the nucleon and can be directly linked to the nucleon tensor charge and transverse-spin structure.
- Less experimentally constrained than chiral-even counterparts.
- Only appear when the hard scattering amplitude contains a chiral-odd partner (twist-3 meson distribution amplitude, transverse meson exchange, etc.)

Nucleon Polarization	Quark Polarization: Unpolarized (U)	Quark Polarization: Longitudinally Polarized (L)	Quark Polarization: Transversely Polarized (T)
U	H		$2\widetilde{H}_T + E_T$
L		$\widetilde{H}$	$\widetilde{E}_T$
T	E	$\widetilde{E}$	$H_T, \widetilde{H}_T$

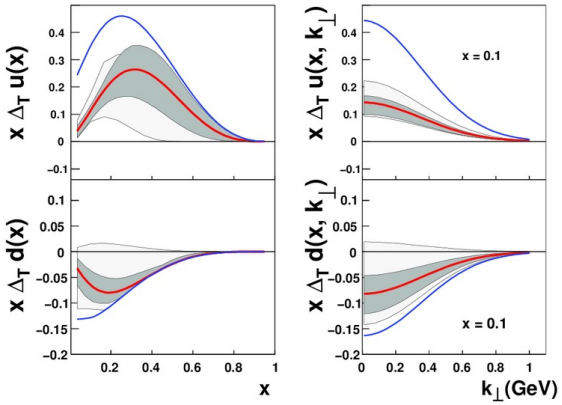
Transversity Tomography



V. Kubarovsky, IWHSS/QCD-N 2025 (2025).

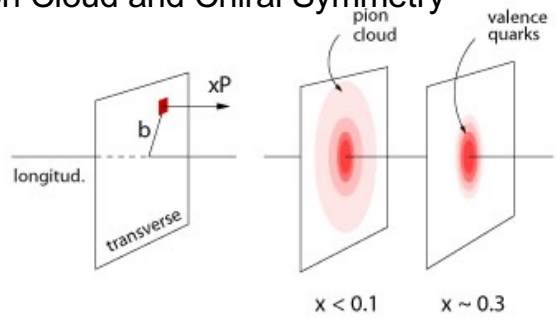
- Access to transversity/tensor charge
- Tensor charge is a key constraint in BSM searches (e.g. β decay, supersymmetry, leptoquarks etc.)

Flavor Separation



H. Gao, The European Physics Journal, Vol 126, 2 (2011).

Pion Cloud and Chiral Symmetry



Nucleon tomography

- Access to the pion cloud through the pion pole term;
- Dependent on the pion-nucleon coupling and long-range structure of the nucleon (flavor asymmetry, nucleon charge radius, axial structure)

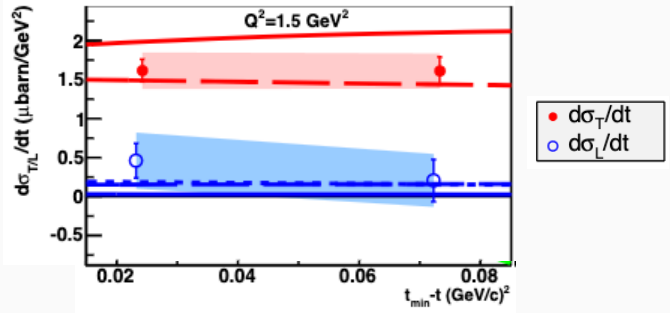
σ_L/σ_T in Pseudoscalar Mesons

Why separate L and T?

- Collinear leading-twist DVMP factorization applies to longitudinal photons.
- At JLab kinematics, π^0 data instead show strong transverse-photon dominance.
- That transverse strength is precisely what makes pseudoscalar DVMP sensitive to chiral-odd / transversity GPDs.

Published π^0 Rosenbluth separation

- Hall A E07-007: $x_B = 0.36$, $Q^2 = 1.5$–2.0 GeV²
- σ_T dominates, $\sigma_L \rightarrow$ far from the asymptotic longitudinal regime.
- Nonzero σ_{LT} still signals a longitudinal amplitude and transverse–longitudinal interference.



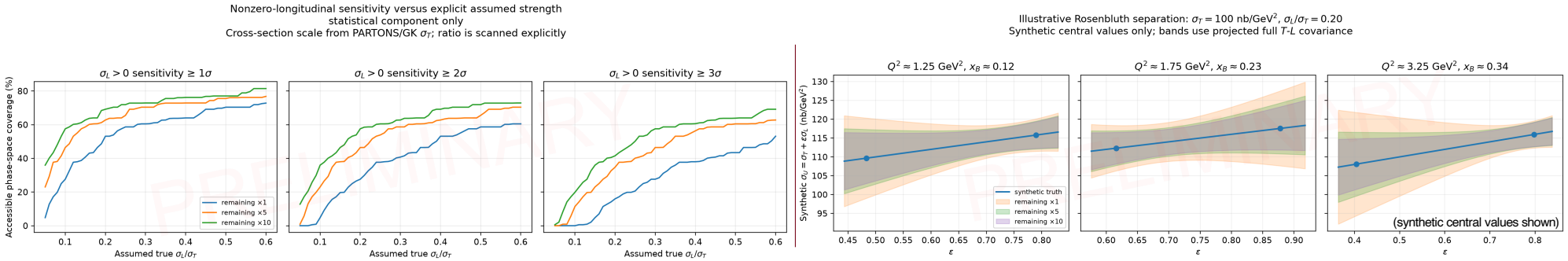
M. Defurne et al., Phys. Rev. Lett. 117, 262001 (2016)

$$\sigma_U(\varepsilon) = \sigma_T + \varepsilon\,\sigma_L \quad \rightarrow \quad \sigma_L \text{ is the slope in } \varepsilon$$

The experimental opportunity: RGA (10.2, 10.6 GeV) + RGK (6.5, 7.5, 8.5 GeV) provide a large ε lever arm at matched kinematics.

Statistical Reach of CLAS12 for π^0

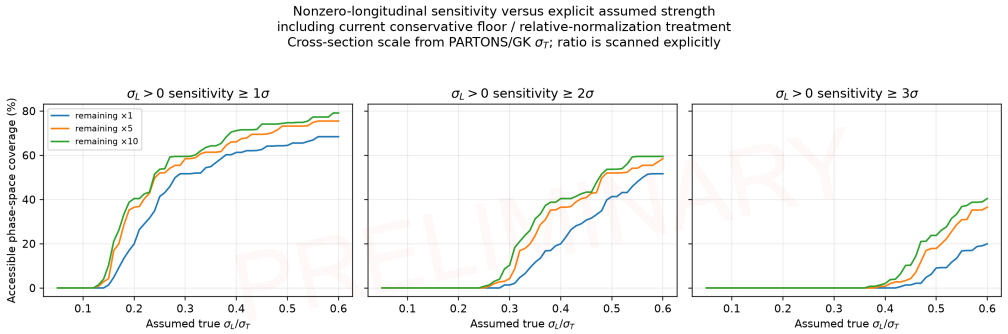
- Simplified L/T separation sensitivity test:
  - Start from the existing RGA (10.6 GeV) and RGK (6.5 GeV) cross-section uncertainties in matched (Q^2,x_B,t,ϕ) bins; project the remaining running at 1x, 5x, 10x the present effective statistical yield.
  - Fit the two beam energies simultaneously to $\sigma_U=\sigma_T+\varepsilon\sigma_L$ (together with the measured ϕ harmonics), then propagate the full T–L covariance to $\delta(\sigma_L/\sigma_T)$.

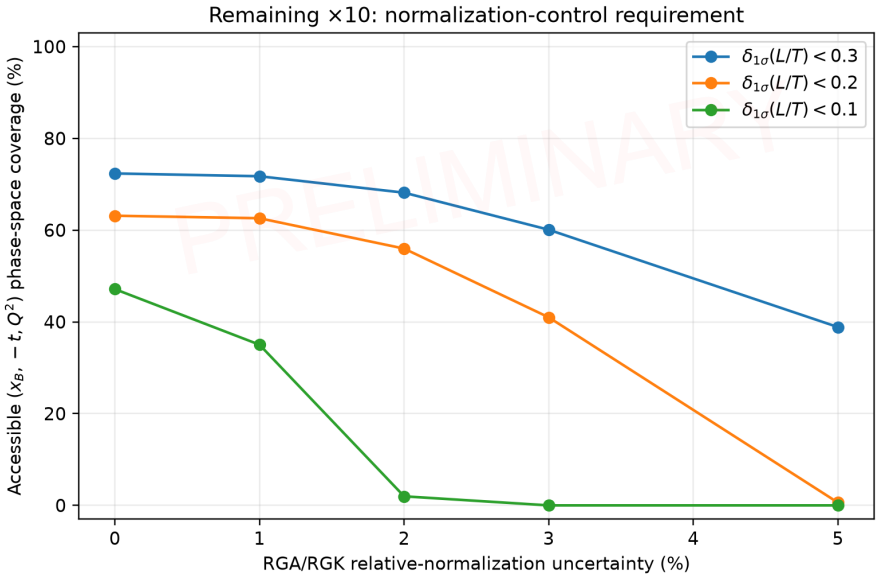


Statistics-only projection: higher effective yield converts the RGA–RGK ε lever arm into broad sensitivity to nonzero σ_L.

Relative Normalization Requirement

But Rosenbluth separation is a difference of absolute cross sections: relative normalization between beam-energy data sets directly limits σ_L.

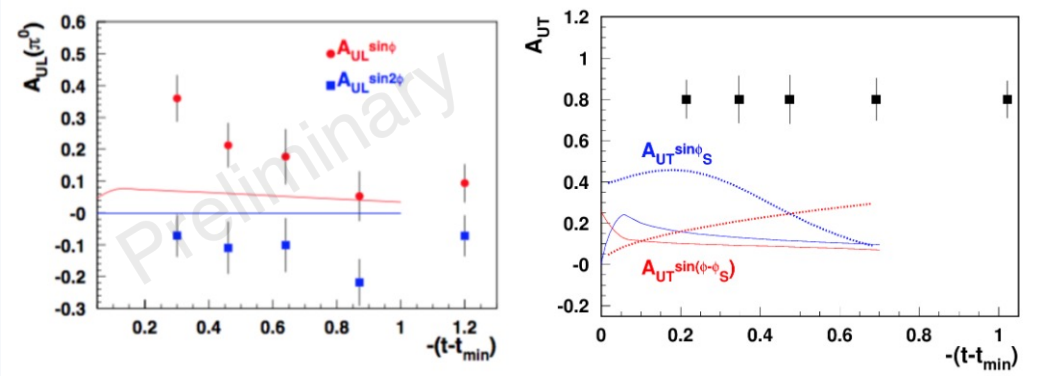




- 1% normalization: much of the statistical reach is retained.
- 2-3% normalization: the aggressive $\delta(L/T) < 0.1$ reach is largely lost.
- 5% normalization: even $\delta(L/T) < 0.2$ becomes limited.

Exclusive π^0 and ρ^0: Completing the Polarized DVMP Program

π^0: RGC longitudinal data → RGH transverse-target projection

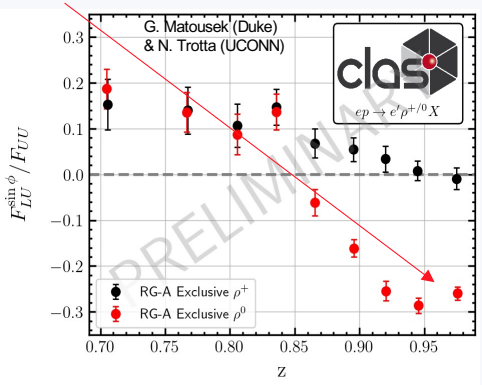


- π^0 provides access to the chiral-odd/transversity sector, including H_T and $\bar{E}_T$.
- Longitudinal and transverse target asymmetries provide complementary interference combinations.
- High-luminosity unpolarized LH_2 data should supply the precision cross-section baseline.

RGH Run-Group Addition E12-11-111A (2025), especially Fig. 13 for π^0 and Sec. 2.1 / Fig. 9 for exclusive ρ^0.

ρ^0: do not leave the vector channel behind

- Longitudinal ρ^0 production gives access to H and E; transverse-target A_{UT} is particularly valuable for E.
- RGC already provides the empirical baseline used for the RGH ρ^0 projections.
- ρ^0 is a crucial physics background for all kinds of SIDIS measurements and interpretations!



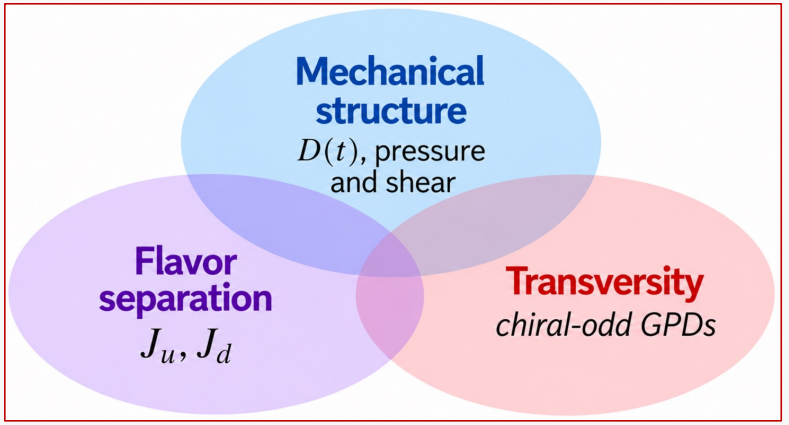
High-L unpolarized cross sections + RGC longitudinal spin + RGH transverse spin = a much more complete meson-GPD program.

Conclusions

High luminosity enables precision measurements.

- Extends DVCS further into the high-Q^2, large |t| region needed to constrain the D-term and improve understanding of mechanical structure.
- Moves neutron and polarized DVCS/DVMP toward genuinely multidimensional measurements that are currently out of reach.
- Enables precision L/T separated DVMP measurements in both the chiral-odd and chiral-even sectors.

A broader and more complete picture of the nucleon.



Luminosity alone is not enough!

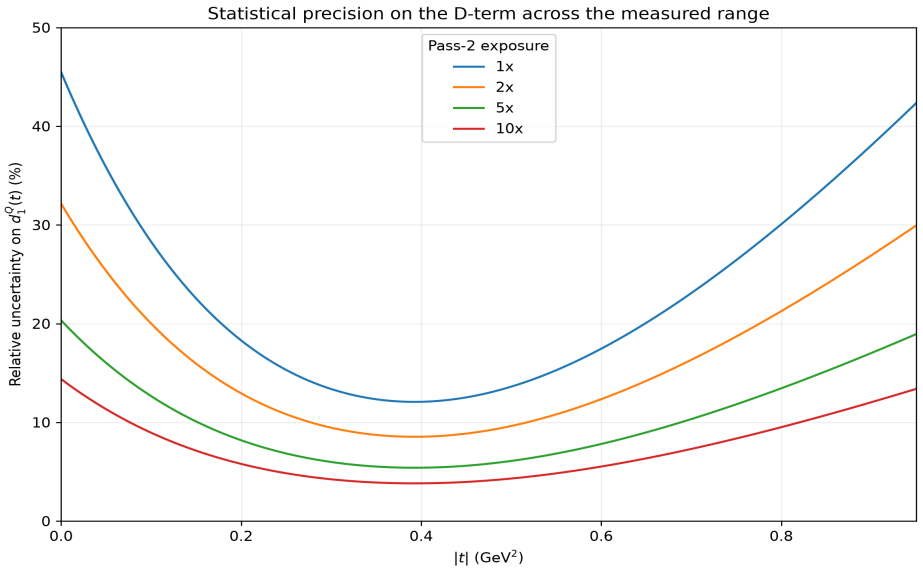
- As statistical precision improves, the limiting uncertainty shifts from event yield to experimental control.
- Realizing the full physics potential in the GPD sector from increased luminosity would require improved control of the normalization and point-to-point systematics.

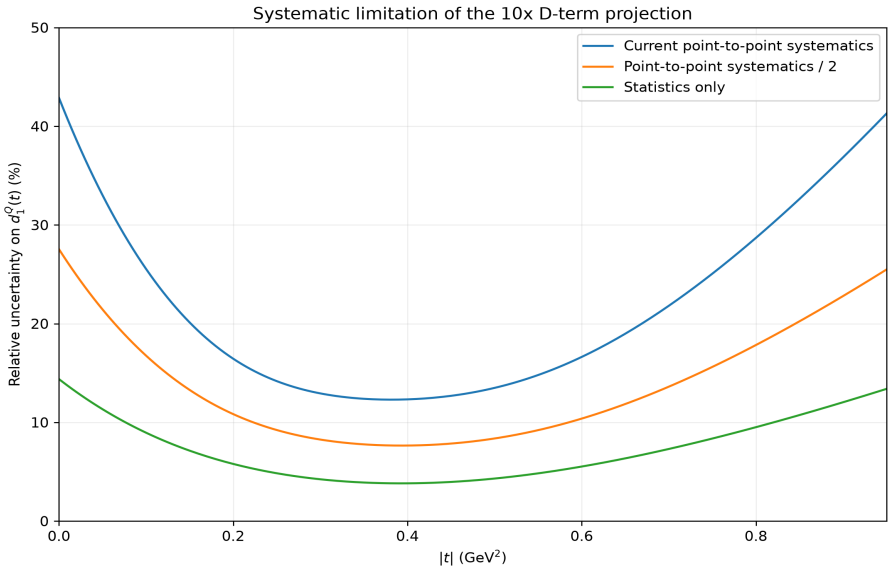
Ancillary Slides

What controls the mechanical-structure precision?

Pressure and shear are derived quantities: they amplify uncertainty in the shape of D(t), not just its overall normalization.

Need simultaneously: t lever arm + statistical precision + controlled point-to-point systematics



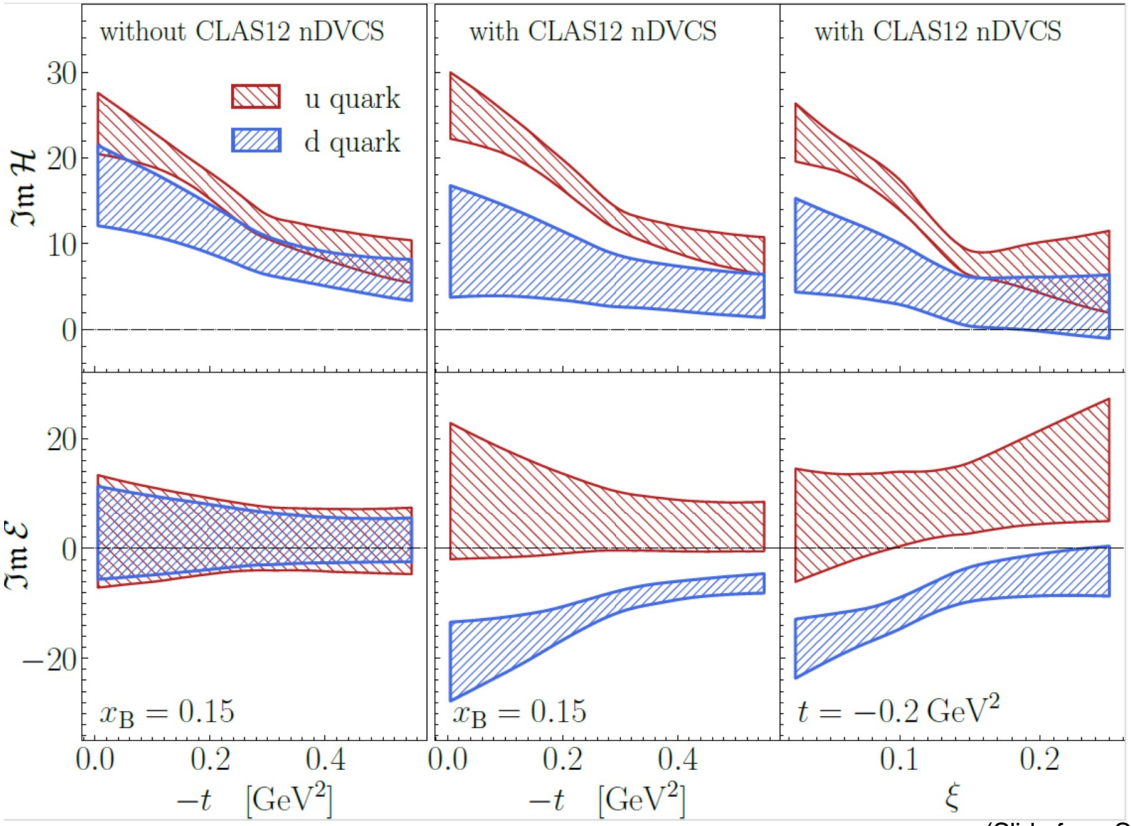


This is why a luminosity upgrade is most valuable when paired with analysis improvements that reduce the present RGA/RGB systematic floor.

Flavor separation of CFFs using the CLAS12 p,n DVCS data

- **Global fits of CFF** using **neural networks (K. Kumericki et al., JHEP 07, 073531 (2011); M. Cuic, K. Kumericki, et al., Phys. Rev. Lett. 533 125, 232005 (2020)**).
- Data used: CLAS6 and HERMES pDVCS observables, CLAS12 pDVCS BSA and nDVCS BSA
- Same extraction method applied to nDVCS Hall-A data, only separation for Im$\mathcal{H}$

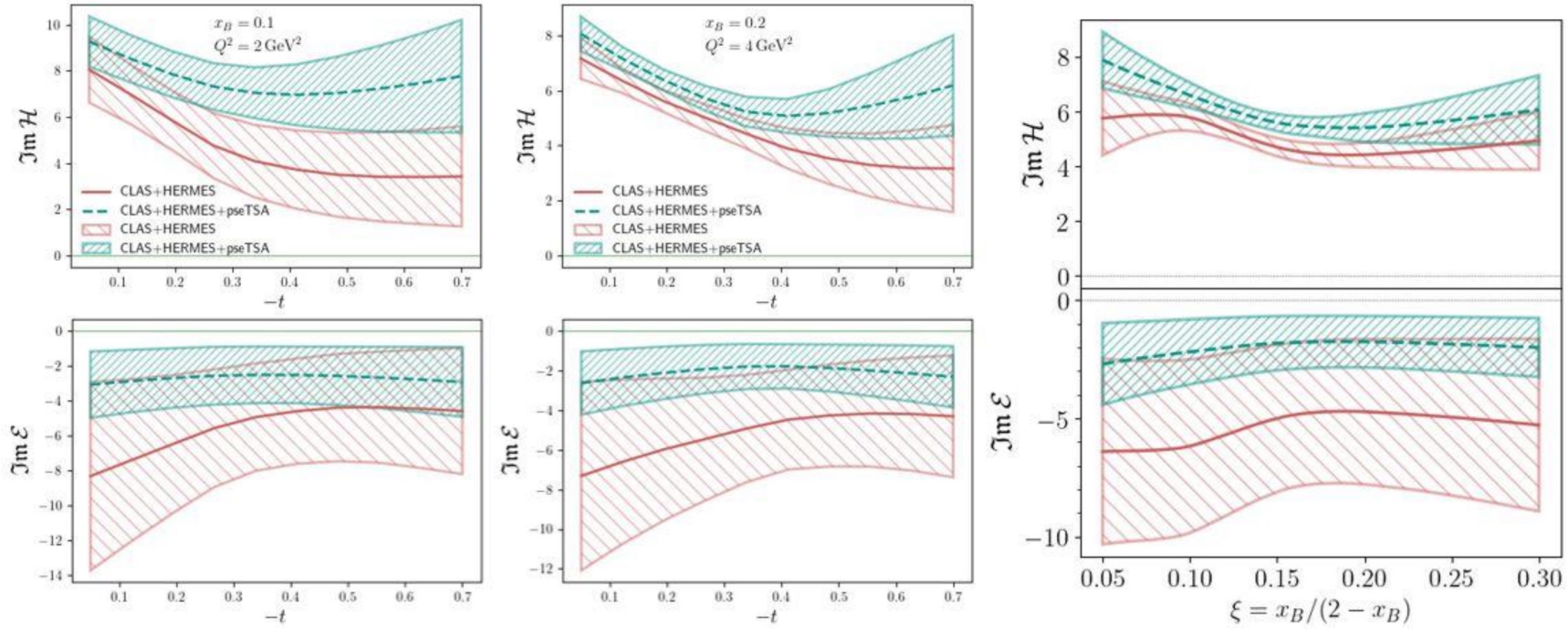
The CLAS12 nDVCS data allow the quark-flavor separation of both Im$\mathcal{H}$ and Im$\mathcal{E}$



(Slide from S. Niccolai)

https://physicsworld.com/a/inner-workings-of-the-neutron-illuminated-by-jefferson-lab-experiment/

Impact of projected pDVCS TTSA from CLAS12 on CFF extraction



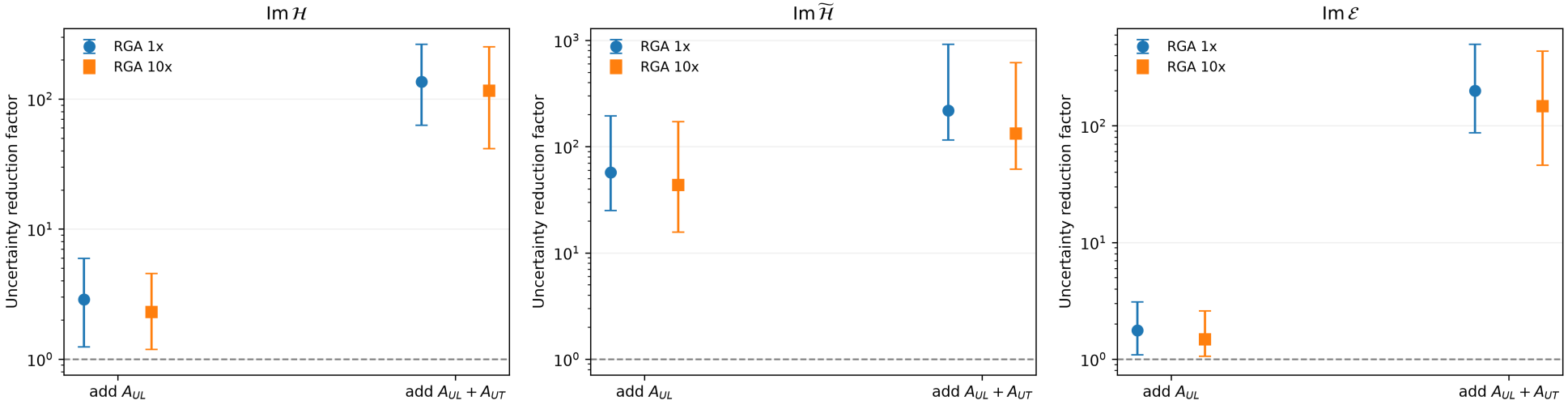
Uncertainty on $Im\mathcal{E}$ will be reduced by a factor of ~3

(Slide from S. Niccolai)

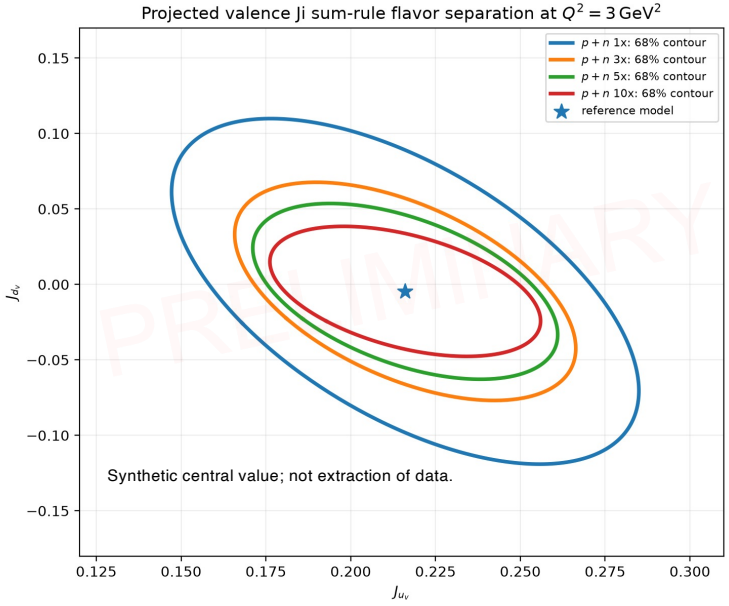
Preliminary analysis by M. Higuera Angulo using the GEPARD framework https://gepard.phy.hr/

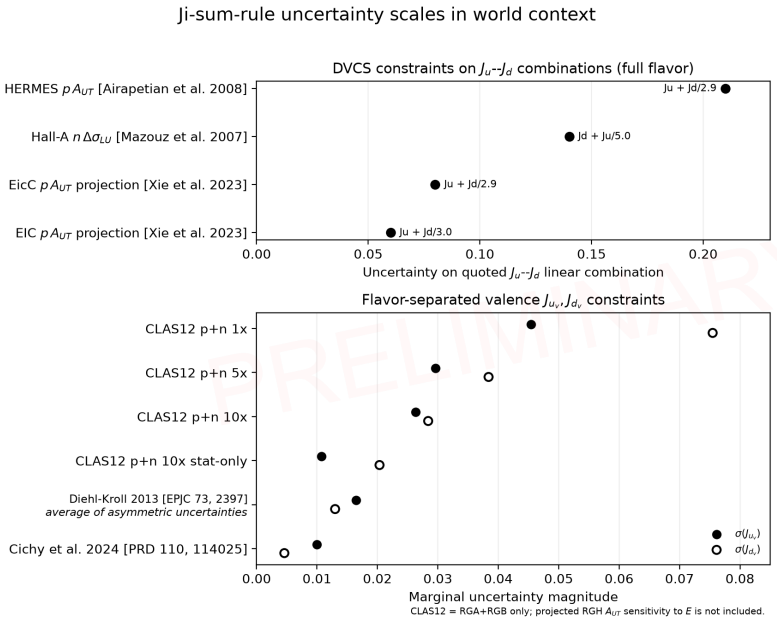
ImH and E?

Polarized observables collapse otherwise unresolved local CFF directions



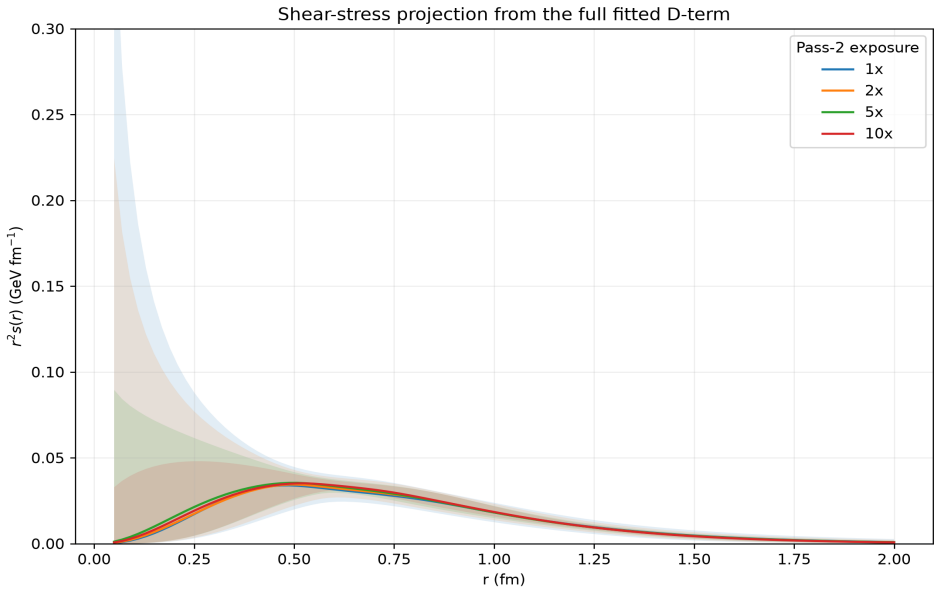
Full local $H + \widetilde{H} + E$ fit. Reduction factor = $\sigma_{\mathrm{XS+BSA}}/\sigma_{\mathrm{added\ observables}}$. Points: median across controlled cells; bars: central 68%. RGC/RGH use nominal completed precision (6× Su22-equivalent).

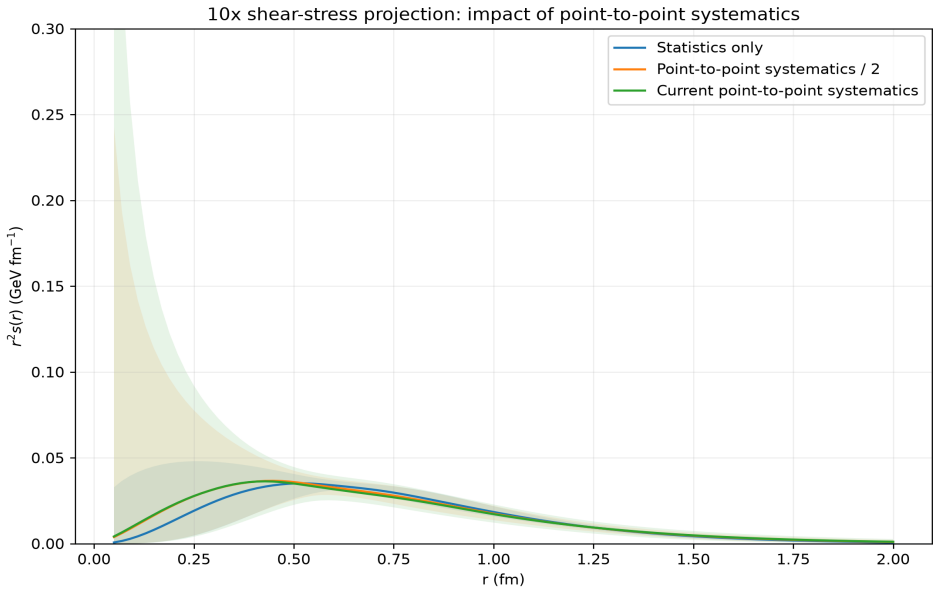

Projected valence Ji sum-rule flavor separation at $Q^2 = 3\,\mathrm{GeV}^2$
$p+n$ 1x: 68% contour
$p+n$ 3x: 68% contour
$p+n$ 5x: 68% contour
$p+n$ 10x: 68% contour
reference model
Synthetic central value; not extraction of data.
J_{u_v}
J_{d_v}
0.15
0.10
0.05
0.00
−0.05
−0.10
−0.15
0.125
0.150
0.175
0.200
0.225
0.250
0.275
0.300


Ji-sum-rule uncertainty scales in world context
DVCS constraints on J_u–J_d combinations (full flavor)
HERMES pA_{UT} [Airapetian et al. 2008]
Hall-A $n\Delta\sigma_{LU}$ [Mazouz et al. 2007]
EicC pA_{UT} projection [Xie et al. 2023]
EIC pA_{UT} projection [Xie et al. 2023]
Ju + Jd/2.9
Jd + Ju/5.0
Ju + Jd/2.9
Ju + Jd/3.0
0.00
0.05
0.10
0.15
0.20
Uncertainty on quoted J_u–J_d linear combination
Flavor-separated valence J_{u_v},J_{d_v} constraints
CLAS12 p+n 1x
CLAS12 p+n 5x
CLAS12 p+n 10x
CLAS12 p+n 10x stat-only
Diehl-Kroll 2013 [EPJC 73, 2397]
average of asymmetric uncertainties
Cichy et al. 2024 [PRD 110, 114025]
$\sigma(J_{u_v})$
$\sigma(J_{d_v})$
0.00
0.01
0.02
0.03
0.04
0.05
0.06
0.07
0.08
Marginal uncertainty magnitude
CLAS12 = RGA+RGB only; projected RGH A_{UT} sensitivity to E is not included.

Shear forces: complementary mechanical information

The same fitted D-term also determines the shear-force distribution, providing an independent view of how internal stresses are spatially organized.



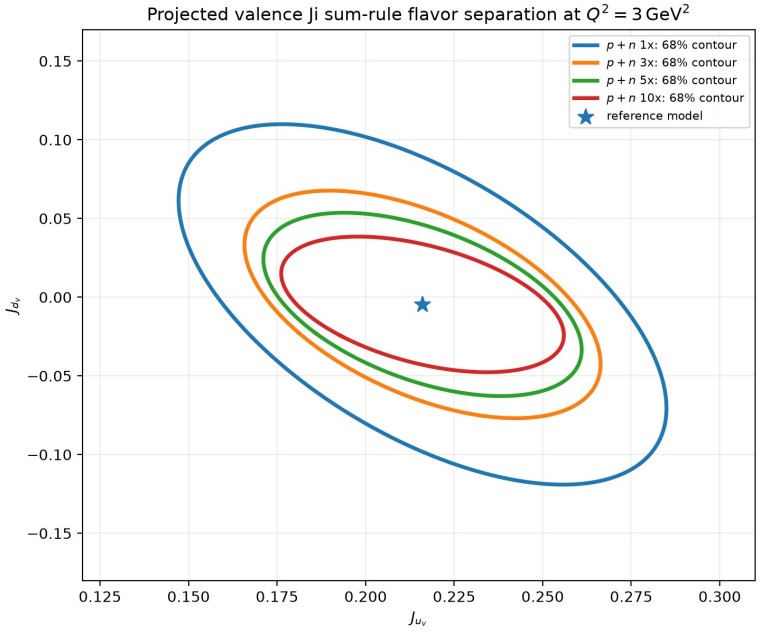


Pressure and shear are therefore not separate measurements: both test whether the extracted D(t) is sufficiently precise and stable for spatial interpretation.

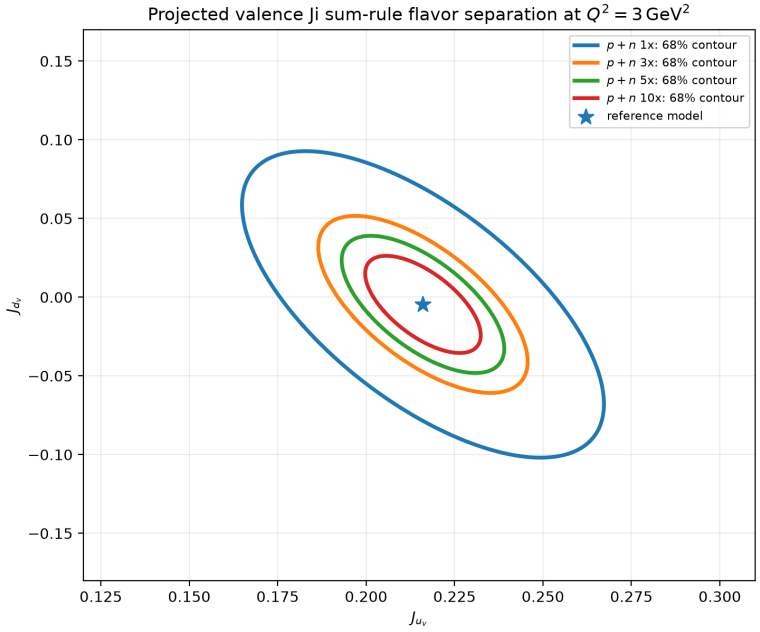
High luminosity only pays off if systematics follow

The same pattern appears in flavor-separated Ji constraints: statistics tighten the contours rapidly, while realistic systematics set the eventual precision floor.

Statistics Only

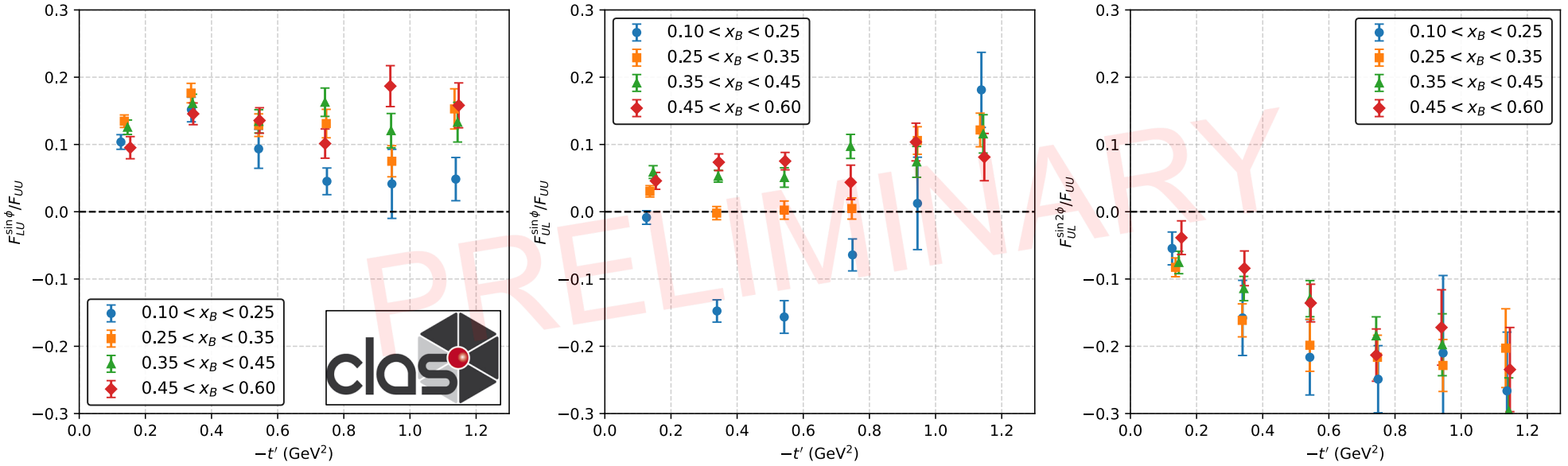


Statistics + Measured RGA/Projected RGB Systematics



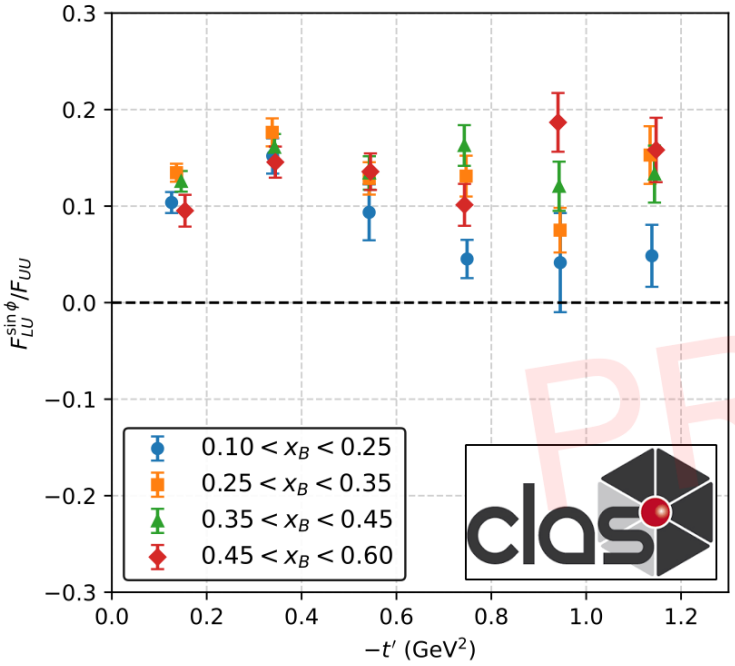
CLAS12 Preliminary

Exclusive π^+ production off a longitudinally polarized NH_3 target.



BSA

Goloskokov & Kroll, Eur. Phys. J. C **65** (2010) 137; [arXiv:0906.0460]



$$A_{LU}^{\sin\phi}\,\sigma_0^M = e_0^2\sqrt{1-\xi^2}\,\frac{\sqrt{-t'}}{2m}\,\mathrm{Im}\Big\{\Big[(1+\eta_M)\,\langle\bar{E}_T^M\rangle_{TL}^* + (1-\eta_M)\,\langle E_T^M\rangle_{TL}^*\Big]\,\langle H_{\rm eff}^M\rangle_{LL}$$

$$+\left[\frac{t'}{2m^2}(1+\eta_M)\,\langle\tilde{H}_T^M\rangle_{TL}^* - 2\,\langle H_T^M\rangle_{TL}^* + \frac{2\xi}{1-\xi^2}\,\langle E_T^M\rangle_{TL}^*\right]\langle E^M\rangle_{LL}\Big\}, \qquad (1)$$

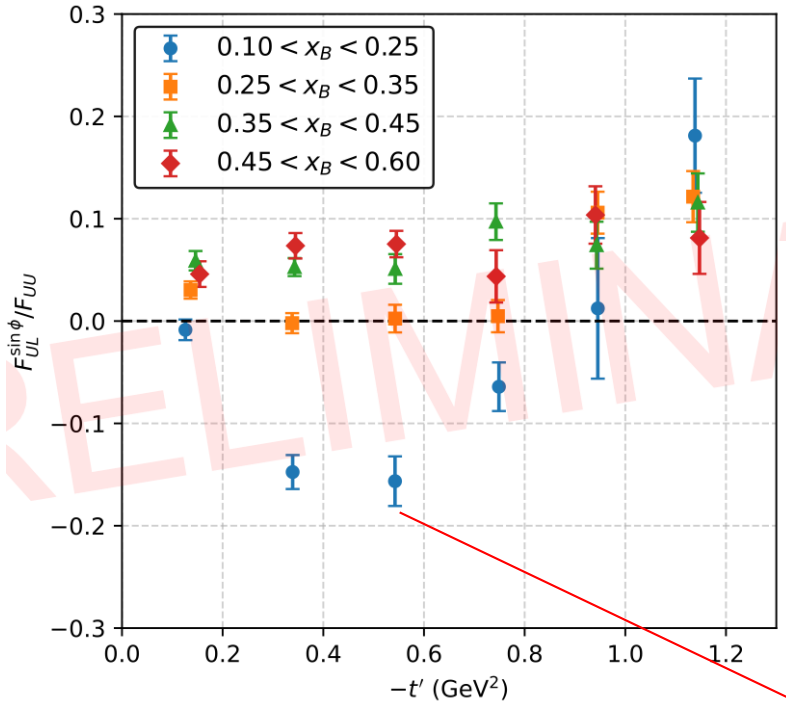
η_M = -1 for pseudoscalar mesons

$$A_{LU}^{\sin\phi}\,\sigma_0^M = e_0^2\sqrt{1-\xi^2}\,\frac{\sqrt{-t'}}{2m}\,\mathrm{Im}\Big\{\underbrace{2\,\langle E_T^M\rangle_{TL}^*}_{3}\,\underbrace{\langle H_{\rm eff}^M\rangle_{LL}}_{1} + \Big[\underbrace{-2\,\langle H_T^M\rangle_{TL}^*}_{4} + \frac{2\xi}{1-\xi^2}\,\underbrace{\langle E_T^M\rangle_{TL}^*}_{3}\Big]\,\underbrace{\langle E^M\rangle_{LL}}_{2}\Big\}, \qquad (3)$$

1) Helicity-conserving longitudinal amplitude built primarily from $\tilde{H}^M$, encodes the quark helicity transverse distribution
2) Nucleon helicity-flip longitudinal amplitude built from $\tilde{\mathcal{E}}^M$; describes how axial charge (helicity density) is displaced when the nucleon flips its spin
3) Describes the transverse shift of quarks with a given transverse spin inside an unpolarized nucleon, analogous to sideways shift from Sivers
4) Generalized transversity GPD (reduces to $h_1(x)$ in the forward limit), encodes information on the correlation between transversely-polarized quarks in a transversely-polarized nucleon

Twist-3 TSA

Goloskokov & Kroll, Eur. Phys. J. C **65** (2010) 137; [arXiv:0906.0460]



$$A_{UL}^{\sin\phi}\,\sigma_0^M = e_0^2\sqrt{1-\xi^2}\,\frac{\sqrt{-t'}}{2m}\,\mathrm{Im}\Big\{\Big[(1-\eta_M)\,\langle\overline{E}_T^M\rangle_{TL}^* + (1+\eta_M)\,\langle E_T^M\rangle_{TL}^*\Big]\langle H_{\rm eff}^M\rangle_{LL}$$

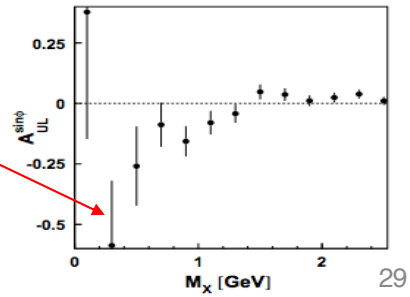
$$+\left[\frac{t'}{2m^2}(1-\eta_M)\,\langle\tilde{H}_T^M\rangle_{TL}^* - 2\,\langle H_T^M\rangle_{TL}^* + \frac{2\xi}{1-\xi^2}\,\langle E_T^M\rangle_{TL}^*\right]\langle E^M\rangle_{LL}\Big\}. \qquad (2)$$

η_M = -1 for pseudoscalar mesons

$$A_{UL}^{\sin\phi}\,\sigma_0^M = e_0^2\sqrt{1-\xi^2}\,\frac{\sqrt{-t'}}{2m}\,\mathrm{Im}\Big\{2\,\underbrace{\langle\overline{E}_T^M\rangle_{TL}^*}_{6}\,\underbrace{\langle H_{\rm eff}^M\rangle_{LL}}_{1} + \Big[\underbrace{\frac{t'}{m^2}\,\langle\tilde{H}_T^M\rangle_{TL}^*}_{5} - 2\,\underbrace{\langle H_T^M\rangle_{TL}^*}_{4} + \frac{2\xi}{1-\xi^2}\,\underbrace{\langle E_T^M\rangle_{TL}^*}_{3}\Big]\,\underbrace{\langle E^M\rangle_{LL}}_{2}\Big\}. \qquad (4)$$

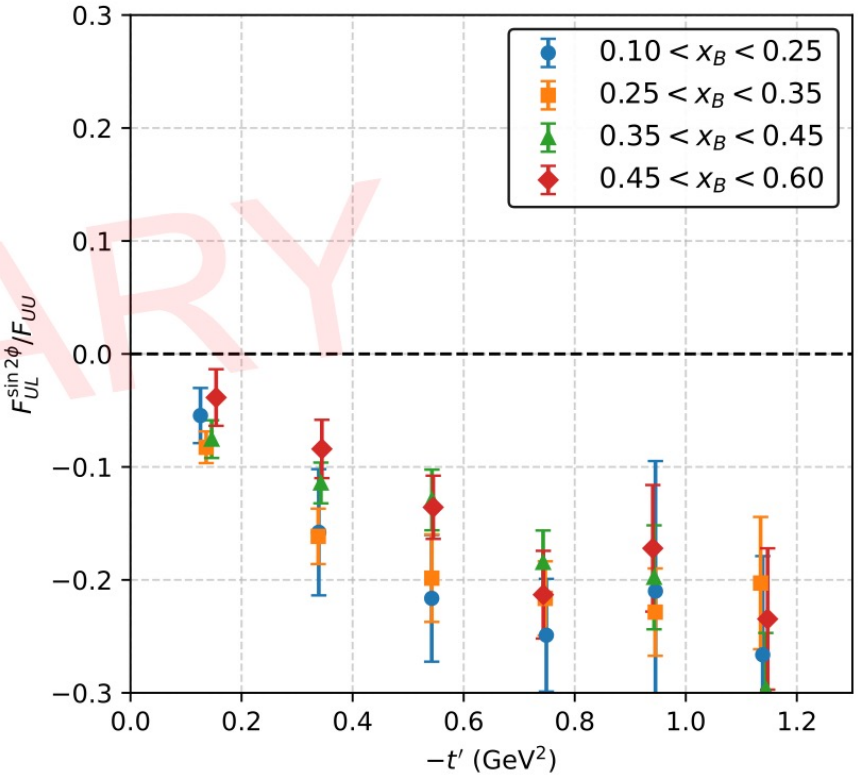
5) Partner to H_T, akin to pretzelosity, associated with quadrupole deformation in the distribution of quark transverse spin when the nucleon is transversely polarized

6) $\overline{E} = 2\tilde{H}_T + E_T$



PRELIMINARY

TT Interference



Goloskokov & Kroll, Eur. Phys. J. C **65** (2010) 137; [arXiv:0906.0460]

$$A_{UL}^{\sin 2\phi}\,\sigma_0^M = -\,e_0^2(1-\xi^2)\,\eta_M\,\frac{t'}{4m^2}\,\mathrm{Im}\left\{\left[\langle H_T^M\rangle_{TL}^* - \frac{\xi}{1-\xi^2}\,\langle E_T^M\rangle_{TL}^*\right]\langle \tilde{H}_T^M\rangle_{TL}\right\},$$

$$A_{UL}^{\sin 2\phi}\,\sigma_0^M = e_0^2\mathcal{P}^2\mathrm{Im}\left\{\left[\langle H_T^M\rangle_{TL}^* - \frac{\xi}{1-\xi^2}\,\langle E_T^M\rangle_{TL}^*\right]\langle \tilde{H}_T^M\rangle_{TL}\right\},$$

- The sin2ϕ TSA is TT interference, built purely from chiral-odd GPDs (as opposed to the LT asymmetries being generated from interference between chiral-even and chiral-odd GPDs).
- Clear nonzero asymmetry indicates nonzero chiral-odd GPDs. In particular:

$$\tilde{H}_T^M \neq 0$$

$$H_T^M - \frac{\xi}{1-\xi^2}E_T^M \neq 0$$

$$\mathrm{phase}\left(H_T^M - \frac{\xi}{1-\xi^2}E_T^M\right) \neq \mathrm{phase}\left(\tilde{H}_T^M\right)$$

- **First observation!**
- π^+ accesses u-d isovector distribution
- u and d quarks show opposite-signed quadrupole anisotropy in transverse spatial distributions

